Experimental Fluid Mechanics Laboratory

Laboratory Coordinator: K. Muralidhar

Associated Faculty Members: Dr(s) Sachin Shinde, P.K. Panigrahi, Pranav Joshi

List of Major Equipment:

- Mach-Zehnder interferometer
- Leica stereomicroscope with computer control
- Ar-Ion laser
- Anton Paar refractometer
- Schlieren and shadowgraph systems
- Stereoscopic PIV
- Micro-PIV with Nd: YAG laser
- Micro-holographic measurement system
- Micro-LIF
- High resolution, color and grey-scale, and high speed CCD cameras
- Precision digital manometer and selection box
- Several clusters and work stations
- Differential Pressure Transducer and flow meter with data acquisition system
- Syringe pump; Gear pump; Ultra-Sonicator
- Mechanical Stirrer; Centrifuge; Magnetic Particle Separator
- Cardio-flow pumps
- Storagescope, high precision multimeter, spectrum analyzer
- Constant temperature baths; Temperature controllers
- Low speed wind tunnel and a Smoke tunnel

Brief description of the laboratory:

The experimental fluid mechanics laboratory utilizes optical measurement techniques for studying flow and thermal fields in a wide range of multi-physics applications. These include evaporation and condensation, bluff body aerodynamics, jets and wakes, and crystal growth. In recent years, two areas being pursued include biomedical imaging in compliant vasculature and interfacial phenomena including electrowetting. Related applications are in disease modeling and production of potable water from a humid environment. Experimental studies are supplemented with numerical simulation and efforts are on to convert basic understanding into meaningful technologies. Fundamental studies related to droplet coalescence, contact line modeling and blood rheology are jointly in progress. Surfaces of interest are superhydrophobic, hydrophobic with high hysteresis and patterned metallic surfaces. Specific interest is towards resolving three dimensionality in the flow distribution and its consequences.

Laboratory research keywords:

Refractive index-based measurements, PIV imaging of cardiovascular flows, interfacial phenomena and contact line modeling, Effect of substrate curvature on drop spreading, electrowetting and electrically actuated droplets, Evaporative cooling

Major Research and Development Contribution of the Laboratory

Year	Major research and development activity
2020-2021	**Contact line dynamics of a water drop spreading over a textured surface in the EWOD configuration -** Modeling the electrowetting process of a liquid droplet placed on a hydrophobic surface in an ambient environment has several challenges over and above those of basic spreading. At an external voltage below the value that causes contact angle saturation, transient spreading is augmented by contact angle reduction defined by the Young-Lippmann equation. In addition, the macroscopic equilibrium contact angle and, therefore, the spreading rate could be altered by the surface hysteresis. Beyond the saturation point, spreading reveals additional features of higher complexity. These details are examined from experiments as well as numerical simulation in the present work. Below the saturation point, the contact angle model developed by the group with the correction related to the electric field is seen to be applicable. Beyond saturation, the experimentally determined instantaneous contact angle distribution shows two distinct functionalities with respect to the contact line velocity. The first prevails from the onset of spreading till the spreading factor attains a peak value. The second trend is initiated with the retraction of the contact line. Except for differences in parametric values, the form of the contact angle model, however, remains unchanged. Simulations in the post-saturation regime are shown to match experimental data in terms of the transient spreading factor, drop shapes, and the instantaneous contact angle. One sponsored project, two doctoral students, four publications, several master's students
2019-2020	**Electrically-driven Continuous Motion of a Liquid Drop on a PDMS-coated Electrode -** Electrically driven continuous motion of a liquid droplet placed on a hydrophobic surface is studied using a single direct current active electrode. While water is mainly the liquid of interest, other liquids such as glycerol, ferrofluids, and a surfactant solution have also been studied. In an experiment, an open electrowetting-on-dielectric (EWOD) configuration is adopted with an active base electrode and a ground wire placed horizontally above but within the drop. Electrohydrodynamic simulations have been carried out in 2D as well as an axisymmetric coordinate system along with a dynamic contact angle model prescribed at the three-phase contact line. Changes in Maxwell's stresses owing to drop deformation and movement are accounted for. With these corrections, experiments and simulations are compared in terms of the interface shapes, contact angles, and instantaneous velocity acquired by the actuated drop and a good match is seen, both, in water and other liquids. Two doctoral students, one post-doctoral fellow, four publications, several Master's students
2018-2019	**Coalescence Characteristics of Liquid Drops on a Hydrophobic Surface with Application to Dropwise Condensation -** Experiments involving two

	small water drops that are placed adjacent to each other on the hydrophobic surface are of interest in the present work. Pendant and sessile configurations are considered and the resulting coalescence process is imaged using a high speed camera. The three-phase contact line of the combined drop remains unpinned and moves in time, while the liquid bridge relaxes with flow taking place from a region of higher to lower pressure. The digital image sequence is analyzed to find the position of the instantaneous center of mass of the drop, whose movement yields the two velocity components. Instantaneous wall shear rates and stresses are thus estimated and compared for various drop configurations. In the present study, appropriate velocity and timescales associated with coalescence are subsequently incorporated in the mathematical model of dropwise condensation. Coalescence experiments are validated against numerical simulation on a variety of surfaces of distinct texture. Heat transfer rates during coalescence are jointly investigated. Differences arising in the condensation patterns owing to coalescence are seen to significant in terms of the condensation rate and the average heat transfer coefficient. Two sponsored projects, two doctoral students, six publications, several Master's students
2017-2018	**Accelerators for Linear Solvers in 3D CFD with Biomedical Applications –** Acceleration techniques to improve the speedup and performance of the solvers of a linear system of equations generated from an unstructured finite volume formulation have been developed. The goal of the study is to devise strategies that accelerate the solution of the matrix system $A\mathbf{x}=\mathbf{b}$ by understanding the matrix properties from the fluid dynamics and the discretization perspective. Matrix properties of pressure, velocity and temperature reveal that those of velocity and temperature remain well-conditioned with condition number near unity. This important result leads to the development of the proposed $\kappa_{G\sigma}$-BiCGSTAB algorithm. When the condition number of the matrix is close to unity the proposed algorithm facilitates switching of a more expensive preconditioner such as the ILU (0) with SGS leading to an overall reduction in simulation time. For pressure, a modified Poisson's equation is derived where the coefficients of the pressure matrix do not change with the changing non-linear velocity field. The pressure matrix is found to be suitable for computing the expensive but highly parallelizable sparse approximate inverse preconditioner. These improvements have been implemented in the context of biomedical fluid flow including a continuum model for the transport of red blood cells in plasma flow inside micro-scale geometries. Two sponsored projects, one doctoral student, two postdoctoral fellows, four publications, several Master's students
2016-2017	**Determination of mass diffusivity of solutions and sol-gel forming colloidal suspensions using interferometry** - Complex fluids such as colloidal glasses and gels exhibit slow dynamics as they cannot achieve thermodynamic equilibrium over practical timescales. They are known for

	their hybrid nature, complex electrostatic interactions between particles and time-dependent structural evolution. They have applications as a rheology modifier in paints, petroleum, cement, cosmetics, health care and the pharmaceutical industry. In the present study, an aqueous suspension of Laponite is used a model suspension in which mutual mass diffusion coefficient is experimentally determined. The measurement technique involves the use of interferometry and shadowgraph. Data extraction from optical images forms a part of the study. These techniques have been validated from mass transfer experiments involving aqueous solutions of NaCl, KCL, glucose and sucrose. New results have been obtained for mass diffusivity of colloidal suspensions of Laponite RD and Laponite JS in water over a range of concentrations and temperature. These are connected to the microstructural dynamics in the suspension and anisotropy of the oblate shaped nanoparticles. A non-monotonic dependence of binary diffusivity on temperature is explained in terms of competing effects arising from thermal energy of Laponite particles, thermal energy of counterions, and the magnitude of charge on Laponite particles that affect their aggregation rate. Two sponsored projects, two doctoral students, seven publications, several Master's students.
2015-2016	**Pulsatile Flow Hemodynamics in Deformed Vasculatures -** Flow imaging in diseased vascular portions in the physiological range of flow rates is experimentally studied. Dynamic similarity is maintained by matching Reynolds number and Womersley number. A blood mimicking fluid mixture is used as a working medium. Temporal characteristics are explored through tracking a neutrally buoyant tracer particle using Particle Tracking Velocimetry (PTV) technique. Two cameras placed orthogonally obtain three components of velocity traces (u, v and w) within the model. Spatial flow characteristics on the medial plane within diseased vascular models are obtained by the Particle Image Velocimetry (PIV) technique. Pulsatile flow is actuated through a cardio-flow pump which ensures the repeatability of the flow waveform for a large number of cycles. Numerical simulations are performed using a finite volume solver and validate experimental results. Simulations provide an insight of three-dimensionality in flow within the model. The goal of the present study is to determine the distributions of hemodynamic indicators such as wall shear stress, time averaged wall shear stress, and oscillatory shear index and their significance in the progression of arterial disease in the short and the long run. Wall compliance and its impact on weakening the vortex strength have been additionally examined. One sponsored project, two doctoral students, five publications, several Master's students.

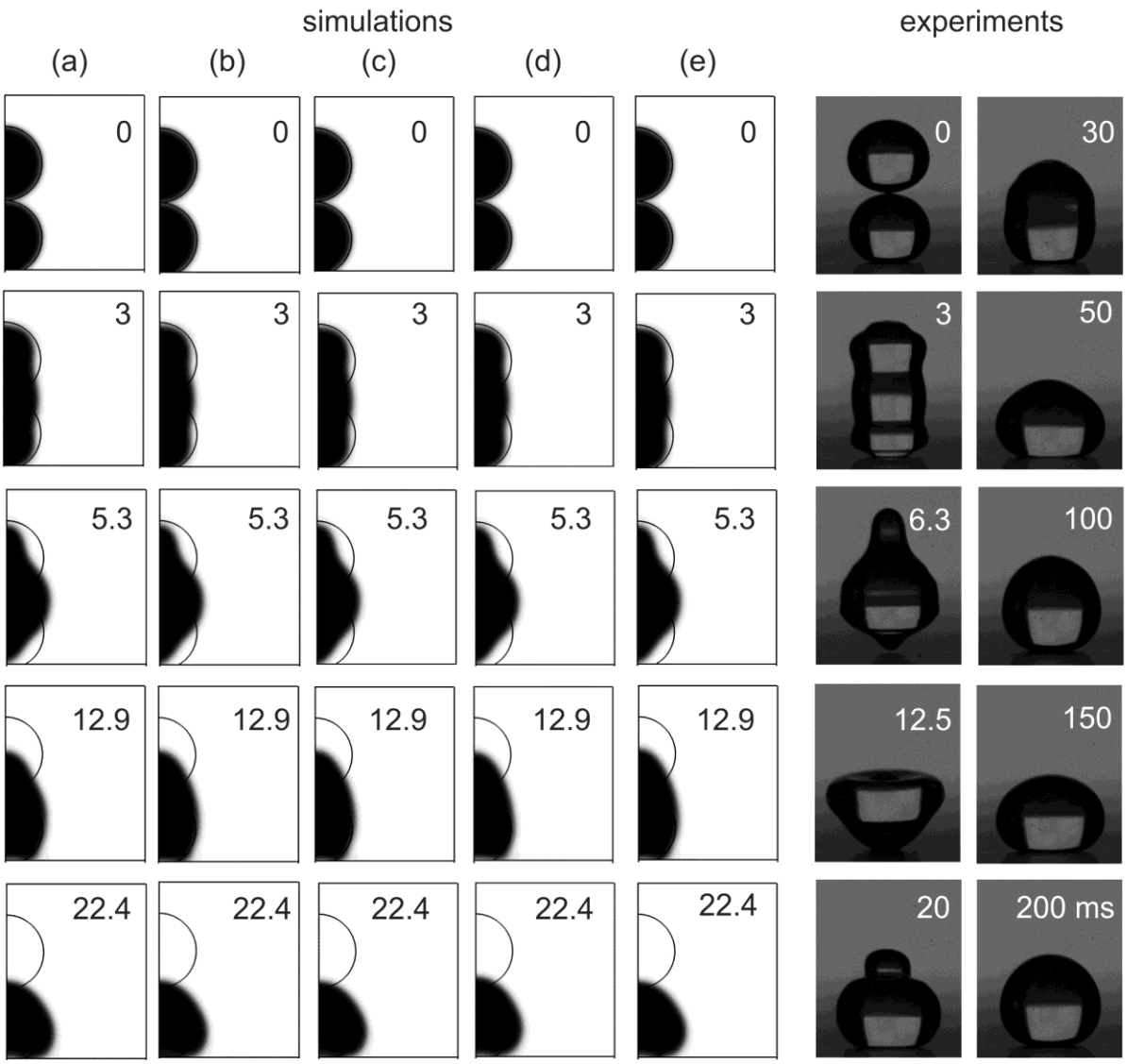

Figure #1: Droplet coalescence Evolution of the simulated interface shapes seen during the coalescence of drops of water using (a) constant contact angle, (b) Bracke et al., (c) Cox (d) Jiang et al., and (e) Kistler models, compared with experiments. Drops are of equal volumes with a combined Bond number of 0.2. The recoil instant is ~ 5.3 ms in simulations and around 6.3 ms in experiments.

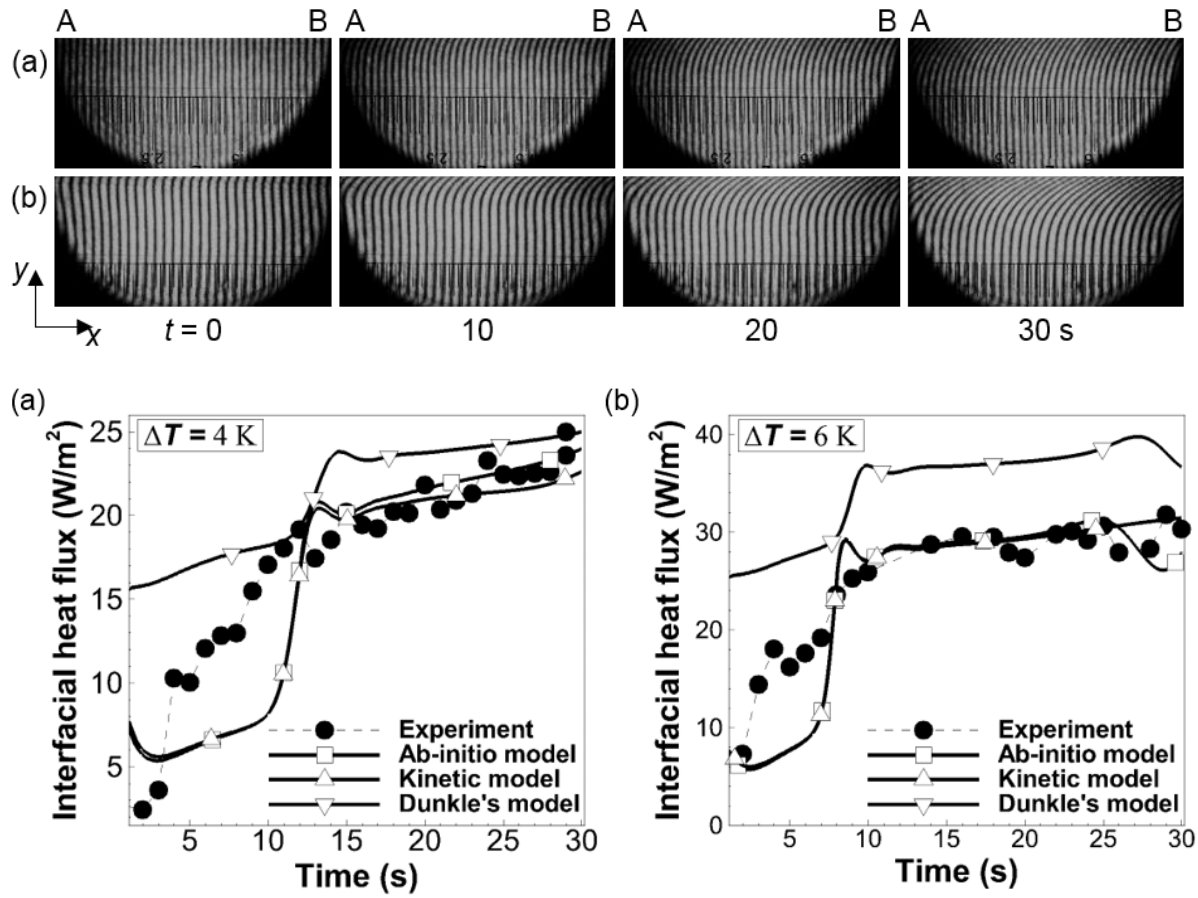

Figure #2: (first row): Evaporative cooling Time-sequence of wedge-fringe interferograms recorded during evaporative cooling of water with the top surface maintained at (a) 294 K (ΔT = 4 K) and (b) 292 K (ΔT = 6 K). The half-filled test cavity and the reference cavity filled with water are initially at 298 K. Both cavities are thermally insulated except the cold surface at the top of the test cavity. Water in the test cavity is filled up to a height of 30 mm while the total cavity height is 60 mm.

Figure #2: (second row): Comparison of the time-dependent average interfacial heat flux obtained from experiments with numerically determined values using three evaporation models. For both experiments and simulations, temperature differences of 4 and 6 K are considered.

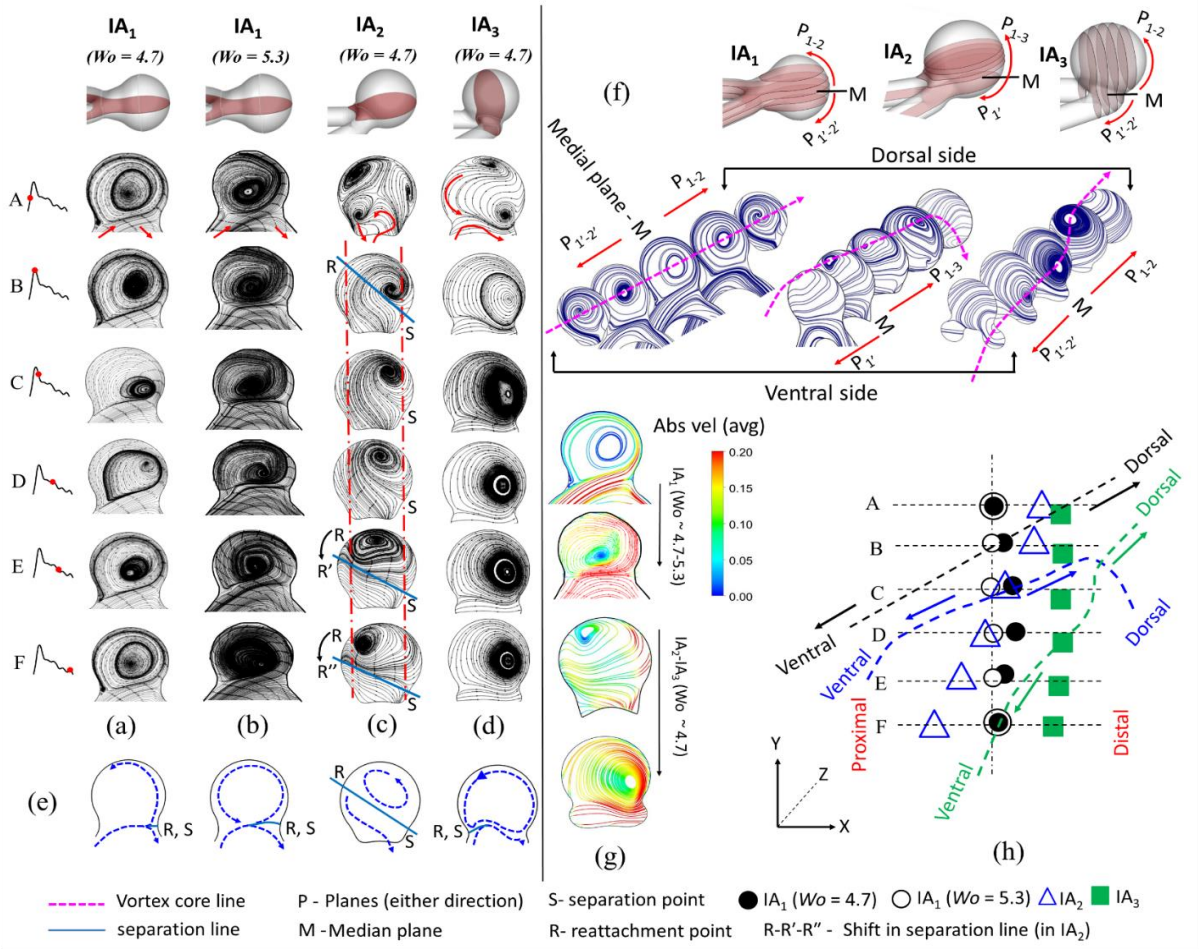

Figure #3: Streamtraces on the medial plane within intracranial models: (a-b) IA_1, (c) IA_2 and (d) IA_3

Figure #3: Biomedical imaging Streamtraces on the medial plane within intracranial models: (a-b) IA_1, (c) IA_2 and (d) IA_3 at phases A-F of the inflow pulsatile waveform. (a, c, d) are numerical and (b) is from the PIV measurement. Arrows (in red) shown in phase A indicate the directions of inflow and outflow. (e) Schematic drawing of typical streamtraces of the time-averaged flow showing the separation point S, reattachment point R, and the separation line joining them. In (c), the reattachment point is seen to move from R to R' and R'' while the separation point is fixed in all the models and phases. (f) Definitions of planes P_1, P_2, P_3, $P_{1'}$ and $P_{2'}$ parallel to the medial plane M for the three models followed by time-averaged streamtraces within the cycle. (g) Contours of the time-averaged absolute velocity in the three models with the PIV measurement included. (h) Spatio-temporal evolution of vortex cores on parallel planes as in (f), moving from the ventral to the dorsal end.

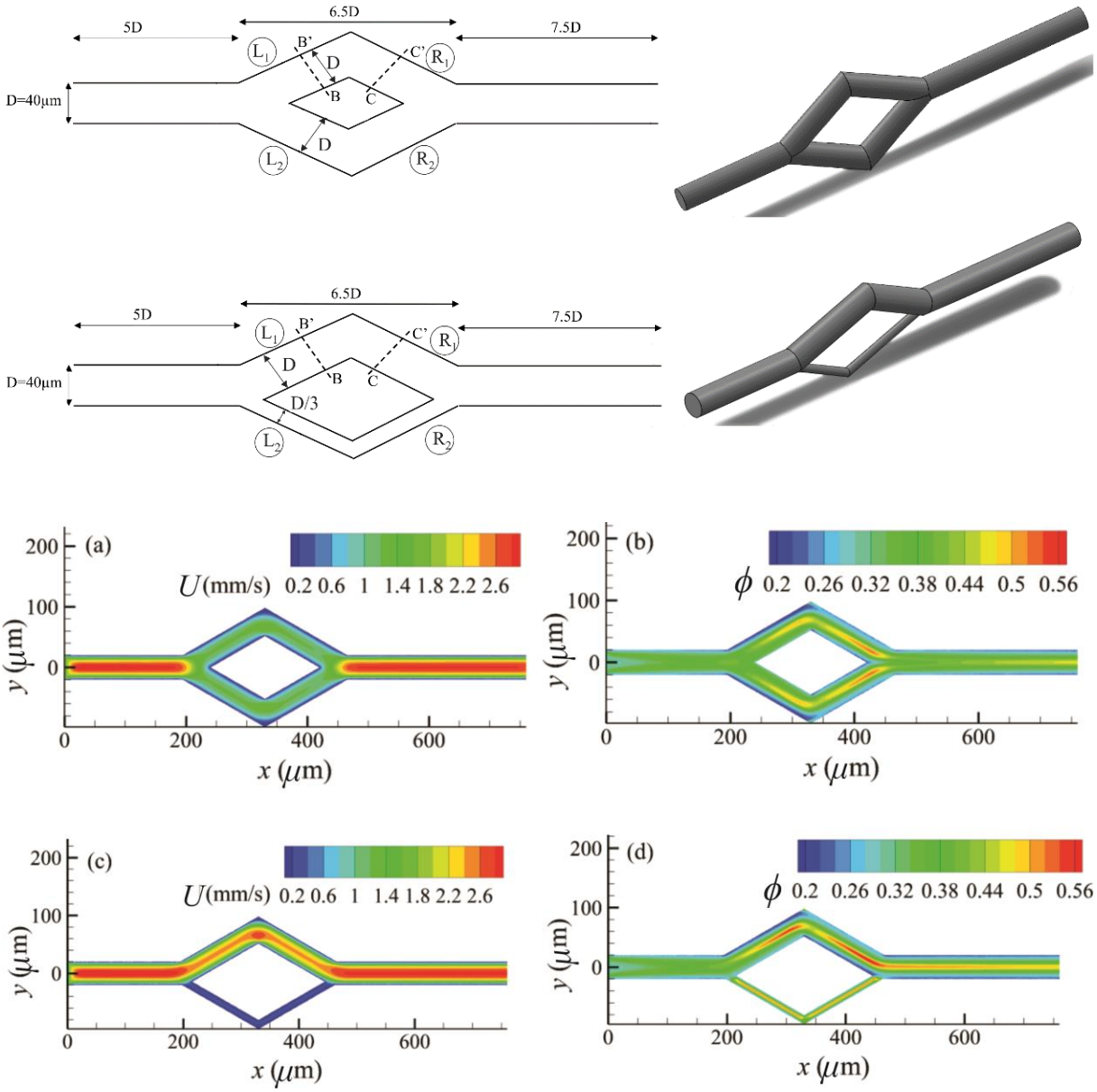

Figure #4: (first row): Blood rheology Layout of tubes with branching selected to demonstrate the Zweifach-Fung bifurcation law. The branching tubes have aspect ratios of 1 and 3 in the geometries above and below respectively.

Figure #4: (second row): Magnitude of the velocity vectors over the mid-plane for aspect ratio (a) *AR*=1 and (c) *AR*=3. RBC concentration over the mid-plane for aspect ratio (b) *AR*=1 and (d) *AR*=3. The average RBC concentration at the inlet is 0.3 while the characteristic shear rate $\bar{\dot{\gamma}} = 40.3\,s^{-1}$ The second row is a confirmation of the Zweifach-Fung bifurcation law which shows that higher concentration of the hematocrit will be realized in the artery of larger diameter.

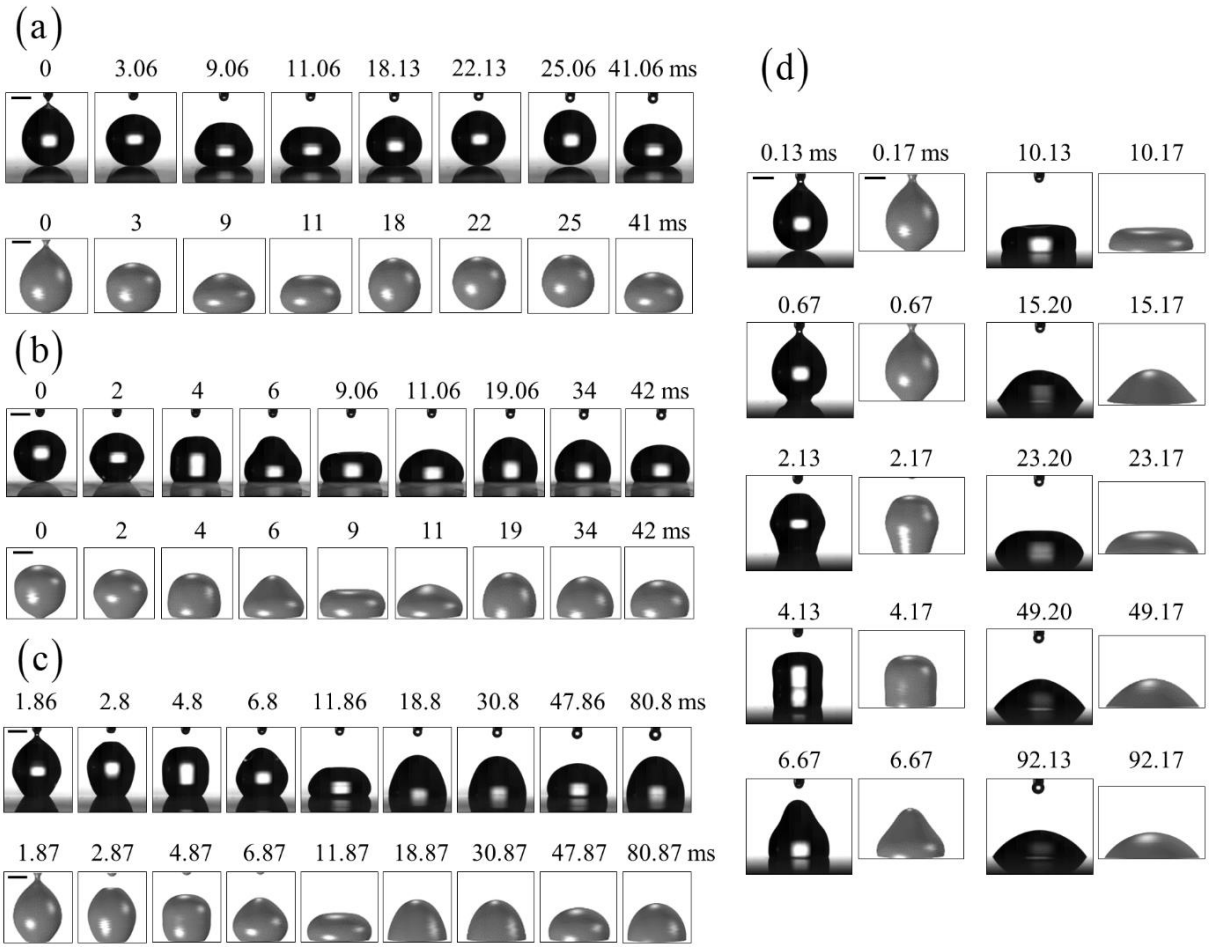

Figure #5: Contact line motion Experiment (black shade) and numerical simulation (grey) of the droplet shape evolution on surfaces of (a) Glaco, (b) FluoroPel, (c) PDMS, and (d) glass. In the numerical simulation, the dynamic contact angle model developed by the group is used as a wetted wall condition. The bars shown in the first image represent a length of 1 mm. The match in terms of the instantaneous drop shapes is seen to be quite good.